Published for SISSA by Springer

Received: March 9, 2017
Revised: April 5, 2017
Accepted: April 6, 2017
Published: April 18, 2017

A light sneutrino rescues the light stop

M. Chala,[a] **A. Delgado,**[b] **G. Nardini**[c] **and M. Quirós**[d]

[a] *Departament de Física Tèorica, Universitat de València and IFIC, Universitat de València-CSIC, Dr. Moliner 50, E-46100 Burjassot (València), Spain*

[b] *Department of Physics, University of Notre Dame, 225 Nieuwland Science Hall, Notre Dame, IN 46556, U.S.A.*

[c] *Albert Einstein Center (AEC), Institute for Theoretical Physics (ITP), University of Bern, Sidlerstrasse 5, CH-3012 Bern, Switzerland*

[d] *Institut de Física d'Altes Energies (IFAE), The Barcelona Institute of Science and Technology (BIST), Institució Catalana de Recerca i Estudis Avançats (ICREA), Campus UAB, 08193 Bellaterra (Barcelona) Spain*

E-mail: mikael.chala@ific.uv.es, antonio.delgado@nd.edu, nardini@itp.unibe.ch, quiros@ifae.es

Abstract: Stop searches in supersymmetric frameworks with R-parity conservation usually assume the lightest neutralino to be the lightest supersymmetric particle. In this paper we consider an alternative scenario in which the left-handed tau sneutrino is lighter than neutralinos and stable at collider scales, but possibly unstable at cosmological scales. Moreover the (mostly right-handed) stop $\widetilde{t}$ is lighter than all electroweakinos, and heavier than the scalars of the third generation lepton doublet, whose charged component, $\widetilde{\tau}$, is heavier than the neutral one, $\widetilde{\nu}$. The remaining supersymmetric particles are decoupled from the stop phenomenology. In most of the parameter space, the relevant stop decays are only into $t\widetilde{\tau}\tau$, $t\widetilde{\nu}\nu$ and $b\widetilde{\nu}\tau$ via off-shell electroweakinos. We constrain the branching ratios of these decays by recasting the most sensitive stop searches. Due to the "double invisible" kinematics of the $\widetilde{t} \to t\widetilde{\nu}\nu$ process, and the low efficiency in tagging the $t\widetilde{\tau}\tau$ decay products, light stops are generically allowed. In the minimal supersymmetric standard model with $\sim 100\,\text{GeV}$ sneutrinos, stops with masses as small as $\sim 350\,\text{GeV}$ turn out to be allowed at 95% CL.

Keywords: Supersymmetry Phenomenology

ArXiv ePrint: 1702.07359

doi:10.1007/JHEP04(2017)097

JHEP04(2017)097

Contents

1 Introduction 1

2 The model and dominant stop decays 4

3 LHC searches and the dominant decays 7
- 3.1 Single channel bounds 9
- 3.2 Combined bounds 11

4 Constraints on particular SUSY models 13

5 Conclusions 15

A Analysis validation 17

JHEP04(2017)097

1 Introduction

In most supersymmetric (SUSY) models, R-parity conservation is implemented to avoid rapid proton decay, which implies that the lightest supersymmetric particle (LSP) is stable. As there are strong collider and cosmological constraints on long-lived charged particles [1–6], the LSP is preferably electrically neutral. This, together with the appealing cosmological features of the neutralino, has had a strong influence on the ATLAS and CMS choice on the SUSY searches. Most of them indeed assume the lightest neutralino to be the LSP or, equivalently for the interpretation of the LHC searches, the long-lived particle towards which all produced SUSY particles decay fast.

Searches under these assumptions are revealing no signal of new physics and putting strong limits on SUSY models. The interpretation of these findings in simplified models provides lower bounds at around 900 and 1800 GeV for the stop and gluino masses, respectively [7, 8], which are in tension with naturalness in supersymmetry. In this sense, the bias for the neutralino as the LSP, as well as an uncritical understanding of the simplified-model interpretations, is driving the community to believe that supersymmetry can not be a natural solution to the hierarchy problem anymore. In the present paper we break with this attitude and take an alternative direction: we assume that *the LSP is not the lightest neutralino but the tau sneutrino*.[1] Moreover we avoid peculiar simplified model assumptions and deal with realistic, and somewhat non trivial, phenomenological scenarios. As we will see, the findings in this alternative SUSY scenario make it manifest the strong impact that biases have on our understanding on the experimental bounds and, in turn, on the viability of naturalness.

[1] For further studies along similar directions, see e.g. refs. [9–12].

As the lightest neutralino is not the LSP, we focus on scenarios with all gauginos (gluinos and electroweakinos) heavier than some scalars. These scenarios, discussed in the context of natural supersymmetry, are feasible in top-down approaches, as e.g. in the following supersymmetry breaking mechanisms.

Gauge mediation.

In gauge mediated supersymmetry breaking (GMSB) [13] the ratio of the gaugino ($m_{1/2}$) over the scalar (m_0) masses behaves parametrically as $m_{1/2}^2/m_0^2 \propto N f(F/M^2)$, where N is the number of messengers, F the supersymmetry breaking parameter and M the messenger mass. The condition $F/M^2 \lesssim 1$ guarantees the absence of tachyons in the messenger spectrum, and if saturated, it yields $f \simeq 3$. In this way, for large N or F/M^2 close to one, the hierarchy $m_{1/2} \gg m_0$ emerges. Within this hierarchy, gluinos are heavier than electroweakinos, and stops heavier than staus, parametrically by factors of the order of g_s^2/g_α^2 at the messenger mass scale M, with g_α being the relevant gauge coupling. The renormalization group running to low scales increases these mass splittings for M much above the electroweak scale. Further enhancements to these mass gaps can be achieved by including also gravity mediation contributions or extending the standard model (SM) group under which the messengers transform [14].[2]

Scherk-Schwarz.

In five-dimensional SUSY theories, supersymmetry can be broken by the Scherk-Schwarz (SS) mechanism [17–25]. In this class of theories, one can assume the hypermultiplets of the right handed (RH) stop and the left handed (LH) third generation lepton doublet localized at the brane, and the remaining ones propagating in the bulk of the extra dimension. In such an embedding, gauginos and Higgsinos feel supersymmetry breaking at tree level while scalars feel it through one-loop radiative corrections. As a consequence, the ratio between the gaugino and scalar masses is $m_{1/2}^2/m_0^2 \propto 4\pi/g_\alpha^2$. Eventually, gluinos and electroweakinos are very massive and almost degenerate, while the RH stops are light but heavier than the LH staus and the tauonic sneutrinos by around a factor g_s^2/g_α^2.

Although the aforementioned ultraviolet embeddings strengthen the motivation of our analysis, in the present paper we do not restrict ourselves to any particular mechanism of supersymmetry breaking. Instead we take a (agnostic) bottom-up approach. We consider a low-energy SUSY theory where the stop phenomenology is essentially the one of the minimal supersymmetric standard model (MSSM) with the lighter stop less massive than

[2] In particular, we assume that the slepton singlet $\widetilde{\tau}_R$ is much heavier than the slepton doublet $(\widetilde{\nu}, \widetilde{\tau})_L$. In GMSB scenarios this hypothesis can be fulfilled only if the messengers transform under a beyond-the-standard-model group with e.g. an extra U(1) such that the extra hypercharge of the lepton singlet is, in absolute value, larger than the one of the lepton doublet. For instance if we extend the SM gauge group by a $\widetilde{\mathrm{U}}(1)$, with hypercharge $\widetilde{Y}$, from E_6 one can easily impose the condition that $\widetilde{Y}(\nu_L) = 0$ while $\widetilde{Y}(\tau_R) \neq 0$ [15, 16]. In this model one needs to enlarge the third generation into the 27 fundamental representation of E_6 decomposed as $27 = 16 + 10 + 1$ under SO(10), while $16 = 10 + \bar{5} + \nu^c$ and $10 = 5_H + \bar{5}_H$ under SU(5). Then we get $4\widetilde{Y} = (-1, 0, -2, 2, 1, -3)$ for the SU(5) representations $(10, \bar{5}, \nu^c, 5_H, \bar{5}_H, 1)$, respectively.

JHEP04(2017)097

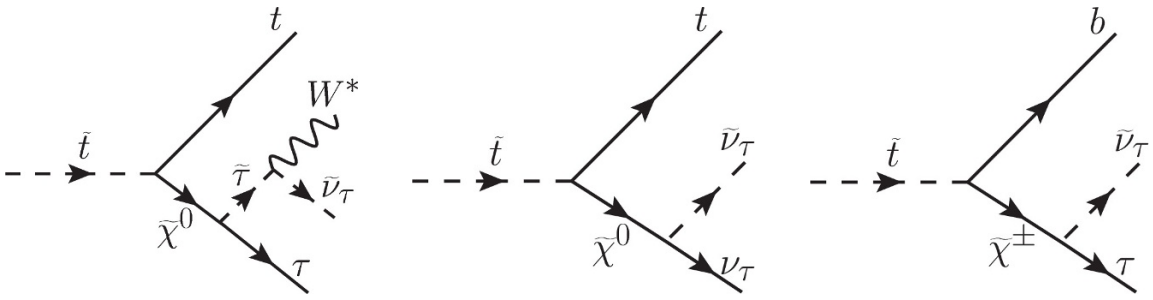

Figure 1. The dominant stop decays in our analysis. Left diagram: production of a top, a tau and a stau, promptly decaying into soft W-boson products and missing transverse energy. Middle diagram: production of a top and two correlated sources of missing transverse energy. Right diagram: production of a bottom, tau and missing transverse energy.

the electroweakinos and more massive than the third-family slepton doublet.[3] This has also been considered in other works (see for example ref. [26]). Gluinos and the remaining SUSY particles are heavy enough to decouple from the collider phenomenology of the lighter stop. In this scenario the LSP at collider scales is therefore the LH *tau sneutrino*. Of course, subsets of the parameter regions we study can be easily accommodated in any of the previously discussed supersymmetry breaking mechanisms or minor modifications thereof.

In the considered parameter regime, the phenomenology of the lighter stop, $\widetilde{t}$, is dominated by three-body decays via off-shell electroweakinos into staus and tau sneutrinos, $\widetilde{\tau}$ and $\widetilde{\nu}$. The viable decay channels are very limited. If the masses of the lightest sneutrino and the lighter stop are not compressed, the only potentially relevant stop decays are $\widetilde{t} \to t\widetilde{\nu}\nu$, $\widetilde{t} \to t\widetilde{\tau}\tau$, $\widetilde{t} \to b\widetilde{\nu}\tau$ and $\widetilde{t} \to b\widetilde{\tau}\nu$, the latter being negligible when the interaction between the lighter stop and the Wino is tiny (see more details in section 2).[4] Thus, for scenarios where the lighter stop has a negligible LH component and/or the Wino is close to decoupling, the relevant stop signatures reduce to those depicted in figure 1. This is the stop phenomenology we will investigate in this paper.

A comment about dark matter (DM) is here warranted. It is well known that the LH sneutrino is not a good candidate for *thermal* DM [27, 28], as it is ruled out by direct detection experiments [29, 30]. Therefore, in a model like the one we study here, one needs a different approach to solve the DM problem. Since many of the available approaches would modify the phenomenology of our scenario only at scales irrelevant for collider observables, incorporating such changes would not modify our results (for more details see section 5).

The outline of the paper is the following. In section 2 we provide further information on the scenario we consider, and on the effects that the electroweakino parameters have on the stop signatures. In section 3 we single out the ATLAS and CMS analyses that, although performed to test different frameworks, do bound our scenario. The consequent

[3] Notice that the mass and quartic coupling of the Higgs do not play a key role in the stop phenomenology. Then, the analysis of the present paper also applies to extensions of the MSSM where the radiative correlation between the Higgs mass and stop spectrum is relaxed.

[4] As a practical notation, we are not differentiating particles from antiparticles when indicating the decay final states.

JHEP04(2017)097

constraints on the stop branching ratios and on stop and sneutrino masses are presented in the same section. The implications for some benchmark points and the viability of stops as light as 350 GeV are explained in section 4. Section 5 reports on the conclusions of our study, while appendix A contains the technical details about our analysis validations.

2 The model and dominant stop decays

In the MSSM and its minimal extensions, it is often considered that naturalness requires light Higgsinos and stops, and not very heavy gluinos. In fact, in most of the ultraviolet MSSM embeddings, the Higgsino mass parameter, μ, enters the electroweak breaking conditions *at tree level*, and only if μ is of the order of the Z boson mass the electroweak scale is naturally reproduced. This however solves the issue only at tree level, as also the stops can *radiatively* destabilize the electroweak breaking conditions. For this reason stops must be light, and the argument is extended to gluinos since, when they are very heavy, they efficiently renormalize the stop mass towards high values. Therefore stops cannot be light in the presence of very massive gluinos without introducing some fine tuning.

Remarkably, the above argument in favor of light Higgsinos, light stops and not very heavy gluinos, is not general. There exist counter examples where the Higgs sector, and thus its minimization conditions, is independent of μ [23–25], and where heavy gluinos do not imply heavy stops [20, 25, 31]. In view of these "proofs of principle", there appears to be no compelling reason why the fundamental description of nature should not consist of a SUSY scenario with light stops and heavy gluinos and electroweakinos. It is thus surprising that systematic analyses on the latter parameter regime have not been performed.[5]

The present paper aims at triggering further attention on the subject by highlighting that the present searches poorly constrain the stop sector of this parameter scenario. For this purpose we focus on the LHC signatures of the lighter stop being mostly RH. The illustrative parameter choice we consider is the one where the stop and slepton mixings are small, and the light third generation slepton doublet is lighter than the lighter stop.[6] The remaining squarks, sleptons and Higgses are assumed to be very heavy, in agreement with the (naive) interpretation of the present LHC (simplified model) constraints. Specifically, these particles, along with gluinos, are assumed to be decoupled from the relevant light stop phenomenology. Moreover, possible R-parity violating interactions are supposed to be negligible at detector scales.

In the present parameter scenario the light stop phenomenology only depends on the interactions among the SM particles, the lighter (mostly RH) stop, the lighter (mostly LH) stau, the tau sneutrino and the electroweakinos. The stop decays into sleptons via off-shell charginos and neutralinos. In principle, due to the interaction between the stop and the neutralinos (charginos), any up-type (down-type) quark can accompany the light

[5] For recent theoretical analyses in the case of light electroweakinos and their bounds see e.g. [32, 33].

[6] These features naturally happen in GMSB and SS frameworks. For GMSB, the trilinear parameter A arises at two loops whereas m_0 appears at one loop. Thus the ratio A/m_0 is one-loop suppressed. Similarly, the SS breaking produces a large tree-level mass for the LH stop and the RH stau fields in the bulk, and generates A at one loop, such that A/m_0 is small due to a one-loop factor. Moreover, the ratio $m_{\tilde{\nu}}/m_{\tilde{t}}$ is parametrically $O(g^2/g_s^2)$ in such GMSB and SS embeddings.

JHEP04(2017)097

stop decay signature. Nevertheless, in practice, flavor-violating processes arise only for a very compressed slepton-stop mass spectrum. For our main purpose, which is to prove that pretty light stops are allowed in the present scenario, the analysis of this compressed region is not essential.[7] To safely avoid this region, we impose $m_{\widetilde{t}} \gtrsim m_{\widetilde{\nu}} + 70\,\text{GeV}$, with $m_{\widetilde{t}}$ and $m_{\widetilde{\nu}}$ being the masses of the lighter stop and the tau sneutrino, respectively.

The kinematic distributions associated to the stop decays strongly depend on the stau and sneutrino masses. In particular, the sneutrino mass $m_{\widetilde{\nu}}$ is free from any direct constraint coming from collider searches and, as stressed in section 1, we refrain from considering bounds that depend on cosmological scale assumptions. On the other hand, numerous collider-scale dependent observables affect the stau as we now discuss.

The ALEPH, DELPHI, L3 and OPAL Collaborations interpreted the LEP data in view of several SUSY scenarios and, depending on the different searches, they obtain the stau mass bound $m_{\widetilde{\tau}} \gtrsim 90\,\text{GeV}$ [1–4]. A further constraint comes from the CMS and ATLAS searches for disappearing charged tracks, for which $m_{\widetilde{\tau}} \simeq 90\,\text{GeV}$ is ruled out if the stau life-time is long [5, 6]. However, in the present scenario with small sparticle mixings, the mass splitting $m_{\widetilde{\tau}} - m_{\widetilde{\nu}}$, given by

$$m_{\widetilde{\tau}}^2 - m_{\widetilde{\nu}}^2 = \frac{\tan^2\beta - 1}{\tan^2\beta + 1}\cos^2\theta_W m_Z^2 + \mathcal{O}(m_\tau^2)\,, \tag{2.1}$$

can be sufficiently large to lead to a fast stau decay, and in fact the charged track LHC bound is eventually overcome for $m_{\widetilde{\tau}} \gtrsim 90\,\text{GeV}$ and $\tan\beta > 1$ (see section 5). On the other hand, a light stau with mass close to the LEP bound modifies the 125 GeV Higgs signal strength $\mathcal{R}(h \to \gamma\gamma)$ unless $\tan\beta \ll 100$ [37]. All together these bounds hint at an intermediate (not very large) choice of $\tan\beta$, as e.g. $\tan\beta \sim 10$.

Finally, a light stau, as well as a light stop, can modify the electroweak precision observables [38]. One expects the corresponding corrections to be within the experimental uncertainties for $m_{\widetilde{\tau}} \gtrsim 90\,\text{GeV}$, $m_{\widetilde{t}} \gtrsim 300\,\text{GeV}$ and negligible sparticle mixing, since the stop is mostly RH and the light stau is sufficiently degenerate in mass with the tau sneutrino. The latter degeneracy plays a fundamental role also in the collider signature of the stau decay: due to the compressed spectrum, the stau can only decay into a stable (at least at detector scales) sneutrino and an off-shell W boson, giving rise to soft leptons or soft jets.

At the quantitative level, the decay processes of the stop are described, in the electroweak basis, by the relevant interaction Lagrangian involving the Bino, Wino, Higgsinos, tau sneutrino, the LH and RH stops and staus ($\widetilde{B}, \widetilde{W}, \widetilde{H}_{1,2}, \widetilde{\nu}_L$, $\widetilde{t}_{L,R}$ and $\widetilde{\tau}_{L,R}$) as well as their SM counter-partners:[8]

$$\begin{aligned}\mathcal{L}_I = &-g\left(\widetilde{t}_L^* b_L \widetilde{W}^+ + \widetilde{\tau}_L^* \nu_L \widetilde{W}^- + \widetilde{\nu}_L^* \tau_L \widetilde{W}^+\right) - \frac{g}{\sqrt{2}}\left(\widetilde{t}_L^* t_L + \widetilde{\nu}_L^* \nu_L - \widetilde{\tau}_L^* \tau_L\right)\widetilde{W}^0 \\ &- \frac{g'}{\sqrt{2}}\left(\frac{1}{3}\widetilde{t}_L^* t_L + \frac{4}{3}\widetilde{t}_R^* t_R + \widetilde{\nu}_L^* \nu_L + \widetilde{\tau}_L^* \tau_L - 2\widetilde{\tau}_R^* \tau_R\right)\widetilde{B}\end{aligned}$$

[7] Notice that in an extreme parameter regime, the stop is long lived and leads to stoponium, whose signatures are qualitatively different from those we are discussing here [34–36]. Including this (small) parameter regime is irrelevant for our purposes, and we thus exclude it from our analysis.

[8] We use two-component Weyl spinor notation for $\psi_{L,R}$, where ψ_L are undotted spinors and ψ_R dotted spinors. By definition $\bar{\psi}_R \equiv \psi_R^\dagger$ are undotted spinors.

JHEP04(2017)097

$$
\begin{aligned}
&-\frac{1}{2}\left\{\frac{h_t}{\sin\beta}\widetilde{t}_R^*\, b_L \widetilde{H}_2^+ + \frac{h_b}{\cos\beta}\widetilde{t}_L \bar{b}_R \widetilde{H}_1^- + \frac{h_t}{\sin\beta}\left(\widetilde{t}_R^* t_L + \widetilde{t}_L \bar{t}_R\right)\widetilde{H}_2^0\right.\\
&\qquad\left.+\frac{h_\tau}{\cos\beta}\left[\left(\widetilde{\tau}_R^*\nu_L + \widetilde{\nu}_L\bar{\tau}_R\right)\widetilde{H}_1^- - \left(\widetilde{\tau}_R^*\tau_L + \widetilde{\tau}_L\bar{\tau}_R\right)\widetilde{H}_1^0\right]\right\}\\
&-i\frac{g}{\sqrt{2}}\left[(\partial^\mu\widetilde{\nu}_L^*)W_\mu^+\widetilde{\tau} + (\partial^\mu\widetilde{\tau}_L^*)W_\mu^-\widetilde{\nu}_L\right] + h.c.\,. \qquad (2.2)
\end{aligned}
$$

Here $h_{t,b,\tau}$ are the SM Yukawa couplings while, following the usual MSSM notation, $\widetilde{H}_2$ ($\widetilde{H}_1$) is the SUSY partner of the Higgs with up-type (down-type) Yukawa interactions. The first two lines in eq. (2.2) come from D-term interactions, the third and fourth lines from F-terms Yukawa couplings and the last line from the covariant derivative of the corresponding fields.

This Lagrangian helps to pin down the Bino, Wino and Higgsino (off-shell) roles in the stop decays. In order to understand the magnitude of the single contributions, it is important to remind that the stop (stau) is mostly RH (LH). Moreover, for our scenario with electroweakino mass parameters M_1, M_2, $\mu \gg m_Z$, the Bino, Winos and Higgsinos are almost mass eigenstates.

The Bino and the electrically-neutral components of Winos and Higgsinos contribute to the decays $\widetilde{t} \to t\widetilde{\tau}\tau$ and $\widetilde{t} \to t\widetilde{\nu}\nu$ (see the first two diagrams in figure 1). We expect different branching ratios into anti-stau tau and into stau anti-tau. This is a consequence of the fact that the decaying particle in the first diagram of figure 1 is a stop and not an anti-stop. This difference in the branching ratios can be understood from the point of view of effective operators obtained in the limit that the neutralinos are heavy enough that can be integrated out. We show that this is so by considering the two (opposite) regimes where the light stop is either mostly RH or mostly LH.

Let us first assume that in the process $\widetilde{t} \to t\widetilde{\tau}\tau$ the decaying stop is RH, i.e. the field $\widetilde{t}_R$ in eq. (2.2). If the neutralinos are mainly gauginos ($\widetilde{B}, \widetilde{W}^0$), as the RH stop is an $\mathrm{SU}(2)_L$ singlet, the process has to be mediated by the Binos. In this case the produced top will be RH and the lowest order (dimension-five) effective operator can be written as $(\widetilde{t}_R^*\widetilde{\tau}_L)(t_R\bar{\tau}_L)$, by which only *staus and anti-taus* are produced, but not anti-staus and taus. For diagrams mediated by Higgsinos, the produced top will be LH and the effective operator is $(\widetilde{t}_R^*\widetilde{\tau}_L)(t_L\bar{\tau}_R)$, and again the stop decay products are staus and anti-taus. However, in the limit of heavy electroweakino masses, the coefficient of the latter operator is suppressed by $\mathcal{O}(v/\mu)$. Now let us instead assume that the decaying stop is LH, that is, $\widetilde{t}_L$ in eq. (2.2). In this case the effective operators for the exchange of gauginos and Higgsinos in $\widetilde{t} \to t\widetilde{\tau}\tau$ would be $(\widetilde{t}_L^*\widetilde{\tau}_R)(t_L\bar{\tau}_R)$ and $(\widetilde{t}_L^*\widetilde{\tau}_R)(t_R\bar{\tau}_L)$ respectively, implying again that the decay products are staus and anti-taus. The contribution to the latter effective operators is small if the RH stau is heavy (and/or the LH component of the stop is small), as happens in the considered model, leading again to the production of *staus and anti-taus* with either chirality.

In reality, in our scenario with mostly RH light stops, since neutralinos are not completely decoupled, full calculations of the stop decays exhibit also some anti-stau and tau contributions. These proceed from dimension-six effective operators such as e.g. $(\widetilde{t}_R^*\partial_\mu\widetilde{\tau}_R^*)(t_R\bar{\sigma}^\mu\tau_L)$, which contain an extra suppression factor $\mathcal{O}(v/\mu, v/M_{1,2})$ with respect to the leading result. We can finally say that the decay of stops is dominated by

JHEP04(2017)097

the production of *anti-taus* while the production of taus is chirality suppressed.[9] Although interesting, this effect escapes from the most constraining stop searches, which do not tag the charge of taus or other leptons (see section 3). For the purposes of the detector simulations the stop branching ratios can thus be calculated without differentiating the processes yielding taus or anti-taus.

The chirality suppression is instead crucial for the three-body decays via off-shell charginos. In principle both decays $\widetilde{t} \to b\widetilde{\tau}\nu$ and $\widetilde{t} \to b\widetilde{\nu}\tau$ are allowed but, due to the chirality suppression, only the latter (which corresponds to the third diagram in figure 1) can be sizeable in our scenario. Indeed, let us consider the case where the stop decaying into b_L and an off-shell charged Higgsino is the RH one.[10] The only five-dimensional effective operator that can be constructed is $(\widetilde{t}_R^* \widetilde{\nu}_L)(b_L \bar{\tau}_R)$ which appears from the mixing between $\widetilde{H}_2^+$ and $(\widetilde{H}_1^-)^*$, after electroweak symmetry breaking, and is thus suppressed by a factor $\mathcal{O}(v/\mu)$. Now instead assume that the stop is LH. At leading order, the decay into b_L and $\widetilde{W}^+$ gives rise to the operator $(\widetilde{t}_L^* \widetilde{\tau}_L^*)(b_L \nu_L)$.[11] Moreover, the $\widetilde{t}_L$ decay into b_R and $(\widetilde{H}_1^-)^*$ can only be generated by a dimension-six operator which is further suppressed by the (tiny) factor $h_b h_\tau / \cos^2\beta$. Thus, in general, only the decay $\widetilde{t} \to b\widetilde{\nu}\tau$ can be relevant in scenarios where the light stop is practically RH (or the Wino is much heavier than the Higgsinos), as we are considering throughout this work. For this reason the decay $\widetilde{t} \to b\widetilde{\tau}\nu$ is absent in figure 1, that only depicts the relevant decays in our scenario.

In the next section we will study in detail how the present LHC data constrain scenarios with light stops predominantly decaying into $t\widetilde{\tau}\tau$, $t\widetilde{\nu}\nu$ and $b\widetilde{\nu}\tau$, while in section 4 we will provide some parameter regions exhibiting this feature and relaxing the bounds on light stops.

3 LHC searches and the dominant decays

The data collected during the LHC Run II, even at small luminosity, have proven to be more sensitive to SUSY signals than their counterpart at $\sqrt{s} = 8\,\text{TeV}$. Among the searches with the most constraining expected reach, we will be interested in those for pair-produced stops in fully hadronic final states performed by the ATLAS and CMS Collaborations, in refs. [39, 40], respectively, as well as searches for pair-produced stops in a final state with tau leptons carried out by the ATLAS Collaboration in ref. [41]. However, the results provided by these experiments can not simply be used to constrain the signal processes under consideration.

This reinterpretation issue is clear for the decay $\widetilde{t} \to t\widetilde{\tau}\tau$ (see the first diagram in figure 1), as the final state is different from any other final state studied by current searches, in particular with more taus involved. In the $\widetilde{t} \to t\widetilde{\nu}\nu$ decay (see the second diagram in figure 1), the final state, a top plus missing transverse energy E_T^{miss}, coincides with e.g. the one of the $\widetilde{t} \to t\widetilde{\chi}^0$ process, with the neutralino as the LSP studied in refs. [39,

[9] The same effect arises also in the $\widetilde{t} \to t\widetilde{\nu}\nu$ decay (second diagram in figure 1), but the collider signatures of these different products are not relevant, for neutrinos or anti-neutrinos are indistinguishable at colliders.

[10] As $\widetilde{t}_R$ is an $\text{SU}(2)_L$ singlet it cannot decay via a charged gaugino $\widetilde{W}^\pm$.

[11] Notice that in our convention both b_L and ν_L are undotted spinors and thus $b_L \nu_L \equiv b_L^\alpha \widetilde{\epsilon}_{\alpha\beta} \nu_L^\beta$, with $\widetilde{\epsilon}_{\alpha\beta}$ being the Levi-Civita tensor, is Lorentz invariant.

JHEP04(2017)097

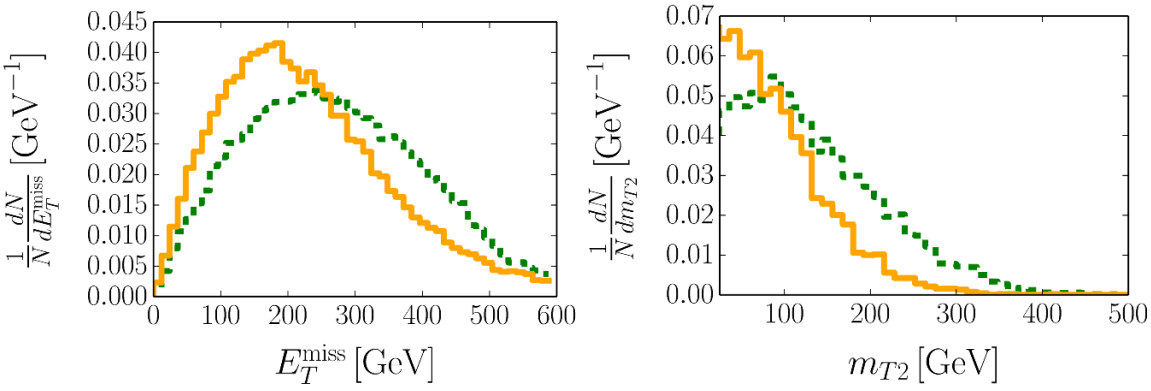

Figure 2. Left panel: normalized distribution of $E_T^{\rm miss}$ in the simplified model of refs. [39, 40] (dashed green line) and our scenario (solid orange line) with BR($\widetilde{t} \to t\widetilde{\nu}\nu$) = 1. In both cases, $m_{\widetilde{t}} = 625\,\text{GeV}$ and $m_{\rm LSP} = 200$ GeV. Right panel: normalized distribution of m_{T2} in the stop decay of the simplified model in ref. [41] (dashed green line) and of our scenario when BR($\widetilde{t} \to b\widetilde{\nu}\tau$) = 1 (solid orange line), with $m_{\widetilde{t}} = 700\,\text{GeV}$ and $m_{\widetilde{\tau}} = m_{\widetilde{\nu}} = 400\,\text{GeV}$ in both cases.

40]. Nevertheless, since the neutralino is *off-shell* in our case, most of the discriminating variables behave very differently, and therefore the experimental bound on $\widetilde{t} \to t\widetilde{\chi}^0$ does not strictly apply [42]. And even the existing analyses for stops decaying into several invisible particles, which also refs. [39–41] investigate, turn out to be based on kinematic cuts with efficiencies that are unreliable in our case. This for instance holds for the $\widetilde{t} \to b\widetilde{\nu}\tau$ decay (see the third diagram in figure 1) whose invisible particle does not exactly mimic the ones of $\widetilde{t} \to b\tau\nu\widetilde{G}$ (where $\widetilde{G}$ is a massless gravitino) analyzed in ref. [41].

For the sake of comparison, in the left panel of figure 2 we show the distributions of $E_T^{\rm miss}$ in the decays $\widetilde{t} \to t\widetilde{\chi}^0$ (dashed green line) and $\widetilde{t} \to t\widetilde{\nu}\nu$ (orange solid line) with $m_{\widetilde{t}} = 625\,\text{GeV}$ and $m_{\rm LSP} = 200\,\text{GeV}$. In the right panel we contrast the shapes of the transverse mass m_{T2} constructed out of the tagged light tau lepton, without any further cut, coming from the decays $\widetilde{t} \to b\widetilde{\nu}\tau$ (dashed green line) and $\widetilde{t} \to b\tau\nu\widetilde{G}$ (orange solid line) for $m_{\widetilde{\tau}} = m_{\widetilde{\nu}} = 400\,\text{GeV}$ and gravitino mass $m_{\widetilde{G}} = 0$. These kinematic variables are of fundamental importance for the aforementioned ATLAS and CMS searches. In particular, as figure 2 illustrates, the stringent cuts on these quantities reduce the efficiency on the signal in our model, with respect to the standard benchmark scenarios for which the LHC searches have been optimized. This issue was previously pointed out in ref. [42].

In the light of this discussion, we recast the aforementioned analyses using home-made routines based on a combination of `MadAnalysis v5` [43, 44] and `ROOT v5` [45], with boosted techniques implemented via `Fastjet v3` [46]. Two signal regions, SRA and SRB, each one divided in three categories, are considered in the ATLAS fully hadronic search [39] (note that SRA and SRB are not statistically independent, though). The different categories vary on the requested amount of $E_T^{\rm miss}$, as well as on the cut on the mass of the tagged fat jets. The CMS fully hadronic analysis [40] considers, instead, a signal region consisting of 60 independent bins. Finally, the ATLAS analysis involving tau leptons carries out a simple counting experiment. Details on the validation of our implementation of

JHEP04(2017)097

	ATLAS [39] (only SRB)	CMS [40]	ATLAS [41]
$\widetilde{t} \to t\widetilde{\tau}\tau$		$\surd$	$\surd^*$
$\widetilde{t} \to t\widetilde{\nu}\nu$	$\surd$	$\surd^*$	
$\widetilde{t} \to b\widetilde{\nu}\tau$		$\surd$	$\surd^*$

Table 1. Analyses employed for testing the different decay modes. The most sensitive one in each case is tagged with an asterisk.

these three analyses can be found in appendix A. We find that our recast of the ATLAS search for stops in the hadronic final state leads to slightly smaller limits, while the ones of the other searches very precisely reproduce the experimental bounds.

Thus, as shown in table 1, we combine the whole CMS set of bins with the above signal region SRB for probing the decay $\widetilde{t} \to t\widetilde{\nu}\nu$, and with the single bin of the ATLAS counting experiment for testing the $\widetilde{t} \to t\widetilde{\tau}\tau$ and $\widetilde{t} \to b\widetilde{\nu}\tau$ processes.[12] Limits at different confidence levels are obtained by using the CL_s method [47]. The expected number of background events, as well as the actual number of observed events, are obtained from the experimental papers. Signal events, instead, result from generating pairs of stops in the MSSM with `MadGraph v5` [48] that are subsequently decayed by `Pythia v6` [49]. The parameter cards are produced by means of `SARAH v4` [50] and `SPheno v3` [51]. When each channel is studied separately, the corresponding branching ratio has been fixed manually to one in the parameter card. When several channels are considered, the amount of signal events is rescaled accordingly.

3.1 Single channel bounds

As discussed in the previous sections, in our scenario the possible decay channels are $\widetilde{t} \to t\widetilde{\tau}\tau$, $\widetilde{t} \to t\widetilde{\nu}\nu$ and $\widetilde{t} \to b\widetilde{\nu}\tau$. In this section we consider each individual decay channel and use the LHC data to bound the corresponding branching ratio in the plane $(m_{\widetilde{t}}, m_{\widetilde{\nu}})$.

The results are reported in figure 3 where, for every given channel, the bounds at the 90% CL (left panels) and 95% CL (right panels) are presented in the plane $(m_{\widetilde{t}}, m_{\widetilde{\nu}})$. Every panel contains the exclusion curves corresponding to several values of the branching ratio into the considered channel. For a given branching ratio, the allowed region stands outside the respective curve (marked as in the legend) and within the kinematically allowed area (below the thin dashed line).

For the decay $\widetilde{t} \to t\widetilde{\tau}\tau$ (upper panels of figure 3) the most sensitive analysis is the ATLAS counting experiment. We combine it with the CMS signal region into a single statistics. As figure 3 shows, the bound on this channel is very weak. In particular, among the searches that we identified as the most sensitive ones to this channel, there is no one constraining this decay mode at 95% CL for $m_{\widetilde{t}} \gtrsim 300\,\mathrm{GeV}$ and $m_{\widetilde{\nu}} \lesssim 100\,\mathrm{GeV}$.

[12] In principle, the two ATLAS analyses could be combined into a single statistics. They are indeed independent, for one of them concentrates on the fully hadronic topology while the other tags light leptons. If we only combine with the CMS analysis is because the validation of this search gives better results. At any rate, no big differences are expected.

JHEP04(2017)097

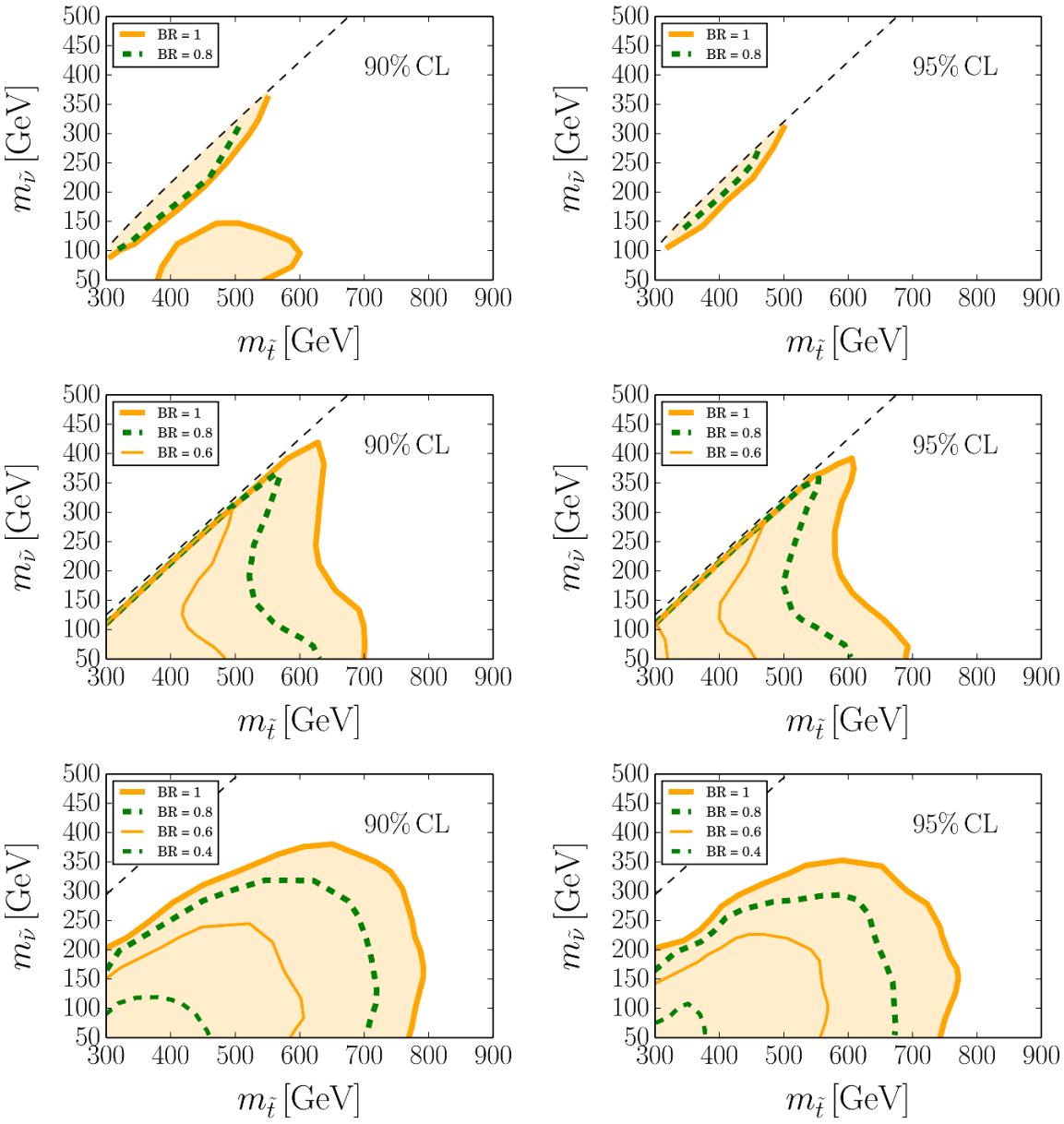

Figure 3. Upper panels: excluded region for BR($\widetilde{t} \to t\widetilde{\tau}\tau$) = 1, 0.8 at the 90% CL (left panel) and 95% CL (right panel) in the plane $(m_{\widetilde{t}}, m_{\widetilde{\nu}})$. For each value of the branching ratio the excluded region is the one enclosed by the corresponding curve. Above the thin dashed line the channel is kinematically forbidden. Middle panels: the same for BR($\widetilde{t} \to t\widetilde{\nu}\nu$) = 1, 0.8, 0.6. Lower panels: the same for BR($\widetilde{t} \to b\widetilde{\nu}\tau$) = 1, 0.8, 0.6, 0.4.

JHEP04(2017)097

For the decay channel $\widetilde{t} \to t\widetilde{\nu}\nu$ (middle panels of figure 3) the most sensitive analysis is the CMS analysis, though the ATLAS search for hadronically decayed stops is also rather constraining. The bound provided in figure 3 is based on the combination of both. As already pointed out, the stringent cuts optimized for the searches for stops into on-shell LSP neutralinos have rather low efficiency on the "double invisible" three-body decay signal involving an off-shell mediator [42].

Finally, the bounds for the $\widetilde{t} \to b\widetilde{\nu}\tau$ decay channel are presented in the lower panels of figure 3. As summarized in table 1, it turns out that the most sensitive analysis to this channel is the ATLAS counting one, although the other two searches can also (slightly) probe this mode. In figure 3, the exclusion curves for this channel are obtained by combining the CMS signal regions with the ATLAS counting one into a single statistics (we do not expect relevant improvements by also including the excluded ATLAS analysis).

We expect the findings to be qualitatively independent of the particular SUSY realization we consider. The only model dependence is the mass splitting between the stau and the sneutrino, which determines the kinematic distribution of the stau decay products. In specific SUSY models such a splitting is determined, and due to the numerical approach of the present analysis, our results are obtained for a concrete stau-sneutrino mass splitting, as detailed in section 4. Nevertheless, in practice, our results should qualitatively apply to all SUSY realizations with prompt decays of staus with mass $m_{\widetilde{\tau}} \lesssim m_{\widetilde{\nu}} + 30\,\text{GeV}$ and $BR(\widetilde{\tau} \to \widetilde{\nu} W^*) \simeq 100\%$.[13]

3.2 Combined bounds

In concrete models, it is feasible that the branching ratios of the three aforementioned stop decay channels sum up to essentially 100%, as we will explicitly see in section 4. In such a situation, we can consider $\text{BR}(\widetilde{t} \to t\widetilde{\nu}\nu)$ and $\text{BR}(\widetilde{t} \to b\widetilde{\nu}\tau)$ as two independent variables, and fix $\text{BR}(\widetilde{t} \to t\widetilde{\tau}\tau)$ as

$$\text{BR}(\widetilde{t} \to t\widetilde{\tau}\tau) = 1 - \text{BR}(\widetilde{t} \to t\widetilde{\nu}\nu) - \text{BR}(\widetilde{t} \to b\widetilde{\nu}\tau) \,. \tag{3.1}$$

It is then possible to use the aforementioned ATLAS and CMS searches to constrain the two-dimensional plane $\big[\text{BR}(\widetilde{t} \to t\widetilde{\nu}\nu), \text{BR}(\widetilde{t} \to b\widetilde{\nu}\tau)\big]$ for some set of values of $m_{\widetilde{t}}$ and $m_{\widetilde{\nu}}$.

The total number of signal events after cuts is given by

$$N = \sum_{i,j} N_{ij}(m_{\widetilde{t}})\ \epsilon_{ij}(m_{\widetilde{t}}, m_{\widetilde{\nu}}) \,, \tag{3.2}$$

with

$$N_{ij}(m_{\widetilde{t}}) = \mathcal{L}\,\sigma(pp \to \widetilde{t}\widetilde{t}^*) \times \text{BR}(\widetilde{t} \to i) \times \text{BR}(\widetilde{t}^* \to j) \,, \tag{3.3}$$

where $\mathcal{L} = 13\,\text{fb}^{-1}$ stands for the integrated luminosity, σ is the stop pair production cross section, and the indices i and j run over the three decay modes. The quantity ϵ_{ij} is the

[13] To clarify this issue, we repeated the $\widetilde{t} \to t\widetilde{\tau}\tau$ simulations for a few parameter points featuring a tiny stau sneutrino mass splitting. For these few points, the constraints on $\widetilde{t} \to t\widetilde{\tau}\tau$ presented in this paper turn out to be comparable, i.e. ruling out a similar region of the parameter space in the plane $(m_{\widetilde{t}}, m_{\widetilde{\nu}})$. Moreover the constraints on $\widetilde{t} \to t\widetilde{\nu}\nu$ and $\widetilde{t} \to b\widetilde{\nu}\tau$ are of course the same. This suggests that the presented bounds can be applied to other scenarios. Extensive parameter space simulations would be however required to prove this feature in full generality.

JHEP04(2017)097

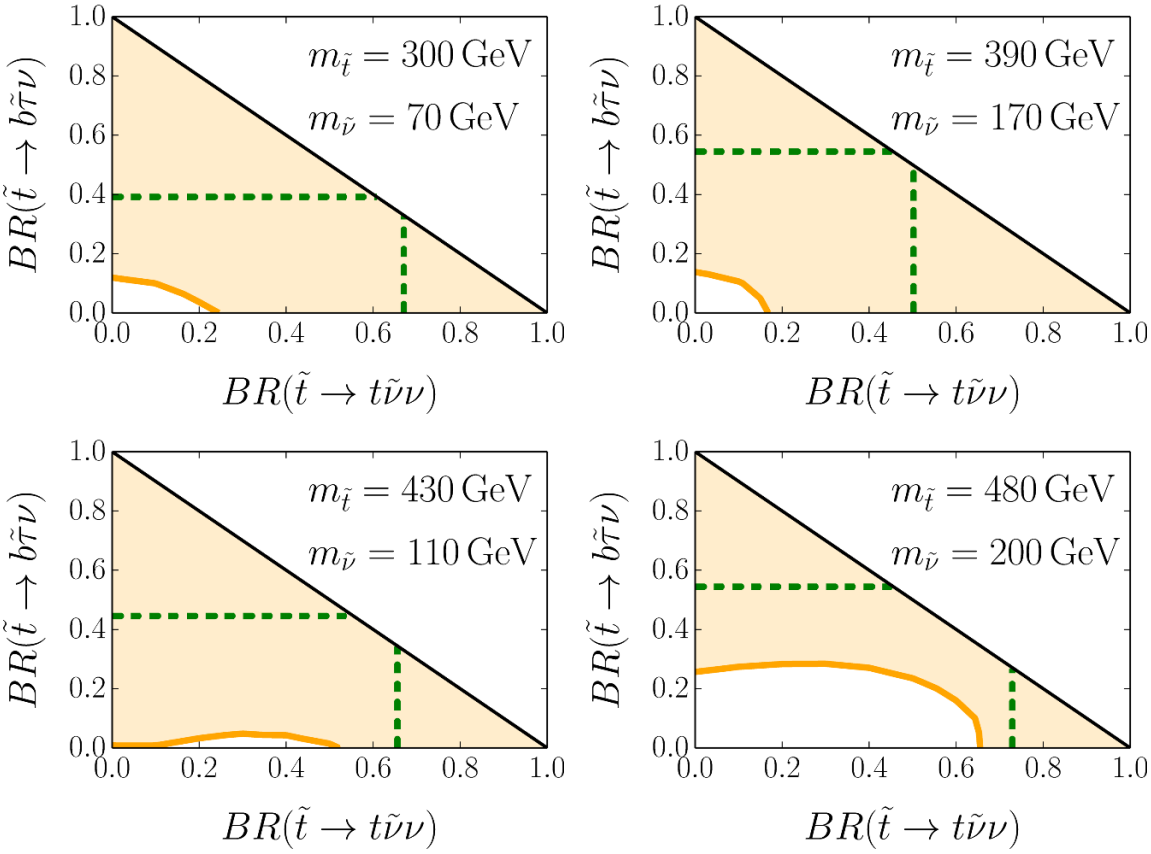

Figure 4. Excluded regions at 95% CL in the plane of BRs for different pairs of $(m_{\tilde{t}}, m_{\tilde{\nu}})$. The areas below (to the left of) the horizontal (vertical) green dashed lines would be allowed if only the $\tilde{t} \to b\tilde{\tau}\nu$ ($\tilde{t} \to t\tilde{\nu}\nu$) mode was considered. The areas enclosed by the orange solid lines are excluded when all channels are combined. The areas above the diagonal black solid straight lines are forbidden by the condition of eq. (3.1).

efficiency that our recast analyses have on the $\widetilde{tt}^* \to ij$ events and is strongly dependent on the mass spectrum. To determine ϵ_{ij} in some given mass spectrum scenarios, we run simulations of $\widetilde{tt}^* \to ij$ following the procedure discussed above. As the searches do not discriminate between ij and its hermitian conjugate, it holds $\epsilon_{ij} = \epsilon_{ji}$.

The results are shown in figure 4. The regions above the horizontal dashed green lines would be the excluded ones had we assumed the signal to consist of only $\widetilde{tt}^* \to b\tilde{\nu}\tau b\tilde{\nu}\tau$ events. Analogously, the areas to the right of the vertical green dashed lines would be the excluded ones under the assumption that only the events $\widetilde{tt}^* \to t\tilde{\nu}\nu t\tilde{\nu}\nu$ are bounded. The regions enclosed by the orange solid lines are instead excluded considering the whole signal, including also the stop decay into $t\tilde{\tau}\tau$ and the mixed channels. For such comprehensive exclusion bounds, a common CL_s is constructed out of the bins in the ATLAS signal region SRB, all bins in the CMS analysis and the single bin in the ATLAS counting experiment.

In light of these results, several comments are in order:

- *i)* The comprehensive bounds, which exclude the region outside the orange curves, are much stronger than those obtained by the simple superposition of the constraints

JHEP04(2017)097

Scenario	M_1	M_2	μ
A	1.1 TeV	5 TeV	5 TeV
B	1.1 TeV	1.1 TeV	1.1 TeV

Table 2. The value of the electroweakino mass parameters assumed in scenarios A and B.

on the isolated signals, ruling out the region above and on the right of the horizontal and vertical dashed lines, respectively. This even reaches points close to the origin, where the main decay channel is $\widetilde{t} \to t\widetilde{\tau}\tau$. The main reason is the inclusion of the mixed channels.

- *ii)* The fact that no single decay necessarily dominates, makes sizeable regions of the parameter space to still be allowed by current data. This is further reinforced by the smaller efficiencies that current analyses have on these processes in comparison to the standard channels. Thus, even small masses such as $m_{\widetilde{t}} \simeq 300\,\text{GeV}$ and $m_{\widetilde{\nu}} \simeq 70\,\text{GeV}$, illustrated in the top left panel, can be allowed.

- *iii)* As we can see from all panels in figure 4, the allowed regions favor large values of $\text{BR}(\widetilde{t} \to t\widetilde{\tau}\tau)$. This effect can be easily understood from the first row plots in figure 3: *there is little sensitivity of the present experimental searches to the channel* $\widetilde{t} \to t\widetilde{\tau}\tau$ when $m_{\widetilde{t}}$ and $m_{\widetilde{\nu}}$ are small.

4 Constraints on particular SUSY models

The results of section 3 can be reinterpreted in concrete SUSY scenarios that exhibit stops decaying as in figure 1, at least at detector scales. The stop, stau, sneutrino and electroweakino mass spectrum and their partial widths are determined by means of `SARAH v4` and `SPheno v3`. More specifically, we use the MSSM implementation provided by these codes, and fix the parameters as follows. We impose $\tan\beta = 10$, in agreement with the arguments of section 2. The slepton and squark soft-breaking trilinear parameters are set to zero. The soft masses of the RH stop, $M^2_{U_R}$, and LH stau doublet, $M^2_{L_L}$, are much lighter than those of their partners with opposite "chirality", $M^2_{Q_L}$ and $M^2_{E_R}$. The electroweakino soft parameters are set, as shown for scenarios A and B in table 2, above the lighter stop mass. The masses of the remaining SUSY particles are not relevant for our analysis, they just need to be heavy enough to not intervene in the stop phenomenology. Nevertheless, for practical purposes, all SUSY parameter have to be chosen and then we set all masses of the SUSY particles except electroweakinos, light stop and light stau doublet at 3 TeV.[14]

[14] As the Higgs plays no role in this study, the origin of electroweak breaking can remain generically unspecified and not used to constrain the SUSY parameters. With the underlying assumption that the Higgs quartic coupling receives a beyond-the-MSSM F or D term contribution, the choice $M^2_{Q_L} \sim (3\,\text{TeV})^2$ is possible in the absence of stop mixing. Otherwise, without beyond-the-MSSM, the observed Higgs mass would be compatible with $M^2_{U_R} \sim (300\,\text{GeV})^2$ and tiny stop mixing only for $M^2_{Q_L} \gg (3\,\text{TeV})^2$ [52], i.e. at the expense of an unpleasant fine tuning.

JHEP04(2017)097

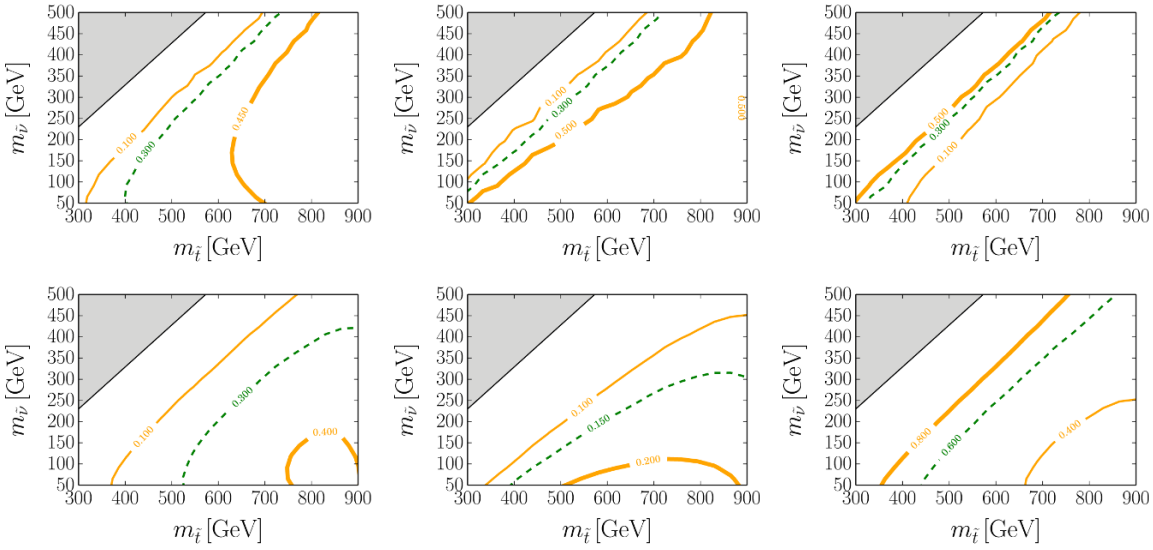

Figure 5. Contour plots of the values of BR($\widetilde{t} \to t\widetilde{\tau}\tau$) (left panels), BR($\widetilde{t} \to t\widetilde{\nu}\nu$) (middle panels) and BR($\widetilde{t} \to b\widetilde{\nu}\tau$) (right panels) in Scenario A (upper panels) and Scenario B (lower panels).

For the above parameter choice, we study two parameter regimes denoted as scenarios A and B, characterized by the values of M_1, M_2 and μ quoted in table 2. Within each regime, we vary the masses $m_{\widetilde{t}}$ and $m_{\widetilde{\nu}}$, by scanning over $M^2_{U_R}$ and $M^2_{L_L}$, and consequently $m_{\widetilde{\tau}}$ is determined as well. We discard the parameter points with $m_{\widetilde{t}} < m_{\widetilde{\nu}} + 70\,\text{GeV}$, which correspond to compressed scenarios that are not investigated in this paper. Contour plots of dominant stop branching ratios are plotted in figures 5 as a function of $m_{\widetilde{t}}$ and $m_{\widetilde{\nu}}$, for scenario A (upper row panels) and scenario B (lower row panels). For each scenario, the branching ratios of $\widetilde{t} \to t\widetilde{\tau}\tau$, $\widetilde{t} \to t\widetilde{\nu}\nu$, and $\widetilde{t} \to b\widetilde{\nu}\tau$ are plotted in the left, middle and right panels, respectively. As anticipated in section 2, the main effect of decreasing M_2 and μ is to enhance $BR(\widetilde{t} \to b\widetilde{\nu}\tau)$, as we can see by comparing the two right panels in figure 5. Conversely, by increasing the value of M_2 and μ we increase the branching ratio corresponding to the channel $t\widetilde{\tau}\tau$, and we expect to make softer the bounds in the plane $(m_{\widetilde{t}}, m_{\widetilde{\nu}})$, in agreement with the general behavior in the lower row panels in figure 3 and in all plots in figure 4. We stress that, within the considered parameter range, the sum of these three branching ratios is always above 95% (depending on the range of $m_{\widetilde{t}}$ and $m_{\widetilde{\nu}}$) which is consistent with our general model assumptions. We also checked numerically that the total width of the stau is $\mathcal{O}(10^{-8}\,\text{GeV})$ for $m_{\widetilde{\nu}} \approx 500\,\text{GeV}$, and is much larger at smaller sneutrino masses. Analogously, the mass gap between the stau and sneutrino masses ranges between $5 - 40\,\text{GeV}$, the latter value appearing for $m_{\widetilde{\nu}} \approx 60\,\text{GeV}$.

The results of section 3, along with the numerical evaluations of the different stop branching ratios, allow to recast the present LHC constraints on scenarios A and B. At each parameter point we rescale the amount of signal events, depending on the values of the branching ratios extracted from the MSSM parameter card corresponding to that point.[15] The final excluded regions at 95% CL in the plane $(m_{\widetilde{t}}, m_{\widetilde{\nu}})$ are shown in figure 6.

[15] In order to check the consistency of our procedure, we also perform the collider simulations described in section 3 for numerous parameter configurations of each scenario. We find perfect consistency, meaning that the contribution from any channel to the search of any other is negligible.

JHEP04(2017)097

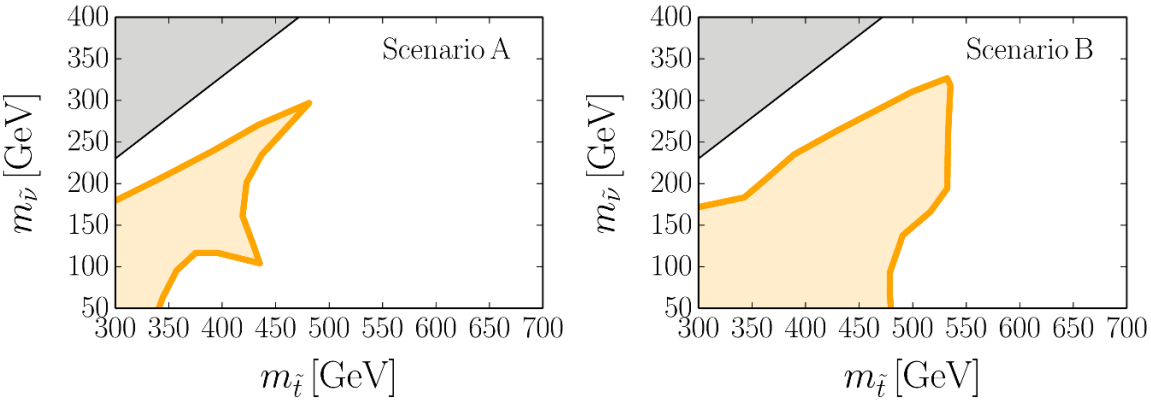

Figure 6. 95% CL exclusion plots (inside the orange lines) for scenario A (left panel) and scenario B (right panel). The gray areas correspond to the region with $m_{\tilde{t}} < m_{\tilde{\nu}} + 70\,\text{GeV}$ that we do not investigate.

Both in scenario A (left panel) and B (right panel) the exclusion bounds (orange areas) are relaxed with respect to their analogous in SUSY scenarios with the neutralino as the LSP. As anticipated, bounds are weaker in scenario A than in scenario B, due the larger values of $\text{BR}(\widetilde{t} \to t\widetilde{\tau}\tau)$. Remarkably, in the presence of light sneutrinos, a RH stop at around 350 GeV is not ruled out by current LHC data, or at least by the ATLAS and CMS analyses performed till now.

5 Conclusions

The bottom line in this paper is that, in the minimal supersymmetric standard model (MSSM) scenario with heavy electroweakinos, light staus and light tau sneutrinos, a mostly right-handed stop with a mass of around 350 GeV is compatible with the present LHC data. This is mostly due to the coexistence of several branching ratios into channels which the LHC searches have weak sensitivity to. Although we have not been concerned about detailed naturalness issues, light stops certainly help in this sense. Heavy electroweakinos are instead considered unnatural, but this is not necessarily true for low scale supersymmetric (SUSY) breaking. In particular, heavy electroweakinos are feasible without inducing a hierarchy problem in some supersymmetry breaking embeddings based on Scherk-Schwarz (SS) and low scale gauge mediated supersymmetry breaking (GMSB) mechanisms.

In the investigated scenario, the light spectrum only includes the Standard Model particles, the mostly right-handed stop, the tau sneutrino and the mostly left-handed stau. Among these SUSY particles, the light stop is heavier than the left-handed stau, which is in turn heavier than the tau sneutrino. The charginos and neutralinos might be at the TeV scale or below, but in any case heavier than the light stop. The number of dominant stop decay channels is only a few. These decays occur via off-shell electroweakinos, and ATLAS and CMS fully hadronic searches for stops into hadronic or tau lepton states [39–41], although designed for a different scope, are the searches that are expected to be most sensitive to them. Remarkably, their constraints do not rule out stops with masses as small

JHEP04(2017)097

as 350 GeV, when the stau mass is around 100 GeV, the sneutrino mass is approximately 60 GeV, and the electroweakinos are at the TeV scale. Neither further bounds do apply: such staus are heavy enough to be compatible with the LEP bounds [1–4], and decay fast, in agreement with the LHC bounds on disappearing tracks [5, 6].

The only constraint comes from cosmological scale observables. In the present study the tau sneutrino is the lightest SUSY particle, stable (at least) at collider scales. If it also is stable at cosmological scales, its thermal relic density is below the dark matter (DM) abundance [27, 28] and, moreover, it is also ruled out by direct detection experiments [29, 30]. So the scenario has to be completed somehow, to provide a reliable explanation of the surveyed DM relic density and/or avoid the strong bounds from direct detection experiments.

There are a limited number of possible mechanisms to circumvent the previous problems without altering the stop phenomenology we have investigated. The simplest possibility is to assume that the sneutrino, even though stable at collider scales, is *unstable at cosmological scales*. In theories with R-parity conservation this can be realized only if there is a lighter SUSY particle (possibly a DM candidate) which the sneutrino decays to, but such that the sneutrino only decays outside the detector and in cosmological times. In theories with GMSB this role can be played by a light gravitino $\widetilde{G}$. It is a candidate to warm DM and its cosmological abundance is given by $\Omega_{3/2}h^2 \simeq 0.1(m_{3/2}/0.2\,\text{keV})$, which suggests a rather low scale of supersymmetry breaking $F \simeq m_{3/2}M_P$. In this case the sneutrino decays as $\widetilde{\nu} \to \nu\widetilde{G}$ and, as far as collider phenomenology is concerned, it looks stable. In theories with a heavy gravitino, as e.g. in theories with SS breaking, one could always introduce a right-handed sneutrino ν_R, lighter than the left-handed sneutrino.[16] On the other hand, the right-handed sneutrino can in principle play the role of DM [9, 12]. If its fermionic partner is light, also the decay $\widetilde{t} \to b\widetilde{\tau}\nu_R$ appears although this process is suppressed by the small neutrino Yukawa coupling. Thus, in practice, the stop collider phenomenology would not be different from that considered in the present paper. Another possibility is if the cosmological model becomes non-standard, as would happen by assuming modifications of general relativity or with non-standard components of DM, as for instance black holes.[17] In this case, in order to overcome the direct detection bounds, the initial density of sneutrinos in thermal equilibrium should be diluted by some mechanism, as e.g. an entropy production (or simply a non-standard expansion of the universe), before the big bang nucleosynthesis [57, 58]. Finally the simplest solution to avoid the direct detection bounds is if there is a small amount of R-parity breaking and the sneutrino becomes unstable at cosmological scales. For instance one can introduce an R-parity violating superpotential as $W = \lambda_{ijk}L_iL_jE_k$ [59], with a small Yukawa coupling λ_{ijk} such that the sneutrino decays as $\widetilde{\nu} \to e_j\bar{e}_k$. Depending on the value of the coupling λ the sneutrino can decay at cosmological times. Needless to say, in this case one would need some additional candidate to DM.

Remarkably, the present bounds on the stop mass in the considered scenario are so weak that even the complete third-generation squarks might be accommodated in the sub-

[16] This can be achieved for instance by localizing the right-handed neutrino multiplet in the brane and thus receiving its mass from higher order radiative corrections.

[17] For discussions in this direction see e.g. refs. [53–56].

JHEP04(2017)097

TeV spectrum. Indeed, the kinematic effects and the coexistence of multi decay channels responsible for the poorly efficient current LHC searches, should also (partially) apply to the left-handed third-family squarks. The presence of these additional squarks in the light spectrum would effectively increase the number of events ascribable to the channels we have analyzed. Nonetheless, since the obtained constraints are very weak, there should be room for a sizeable number of further events before reaching TeV-scale bounds. In such a case, in the heavy electroweakino scenario considered in this paper, present data could still allow for a full squark third-family generation much lighter than what is naively inferred from current constraints based on simplified models. Quantifying precisely this, as well as studying the right-handed neutrino extension, is left for future investigations.

Details aside, our main conclusion highlights the existence of unusual scenarios where very light stops are compatible with the present LHC searches without relying on artificial (e.g. compressed) parameter regions. It is not clear whether this simply occurs because of lack of dedicated data analyses. *In summary, the possibility that the bias for the neutralino as lightest SUSY particle have misguided the experimental community towards partial searches, and that clear SUSY signatures are already lying in the collected data, is certainly intriguing.*

Acknowledgments

The work of MC is partially supported by the Spanish MINECO under grant FPA2014-54459-P and by the Severo Ochoa Excellence Program under grant SEV-2014-0398. The work of AD is partially supported by the National Science Foundation under grant PHY-1520966. The work of GN is supported by the Swiss National Science Foundation under grant 200020-168988. The work of MQ is also partly supported by the Spanish MINECO under grant CICYT-FEDER-FPA2014-55613-P, by the Severo Ochoa Excellence Program under grant SO-2012-0234, by Secretaria d'Universitats i Recerca del Departament d'Economia i Coneixement de la Generalitat de Catalunya under grant 2014 SGR 1450, and by the CERCA Program/Generalitat de Catalunya.

A Analysis validation

In order to validate our implementations of the experimental analyses of refs. [39–41], we apply them to Monte Carlo events generated using the same benchmark models of those searches. Specifically, these are pair-produced stops decaying as $\widetilde{t} \to t\widetilde{\chi}^0$ [39, 40] and $\widetilde{t} \to b\overline{\nu}\widetilde{\tau}$ ($\widetilde{\tau} \to \tau\widetilde{G}$) [41]. The signal samples are obtained by generating pairs of stop events in the MSSM with `MadGraph v5` at leading order. Such events are subsequently decayed by `Pythia v6`. In the parameter cards produced with `SARAH v4` and `SPheno v3`, the branching ratio $\mathrm{BR}(\widetilde{t} \to t\widetilde{\chi}^0)$ is fixed manually to 100% in the first two analyses. In the same vein, for the analysis of ref. [41] we fix both $\mathrm{BR}(\widetilde{t} \to b\overline{\nu}\widetilde{\tau}) = 1$ and $\mathrm{BR}(\widetilde{\tau} \to \tau\nu) = 1$. Notice that, in this last case, the neutrino plays the role of the (massless) gravitino, thus mimicking the channel studied in the experimental work. As stated in the main text, bounds are obtained by combining the different bins of a particular search into a single

JHEP04(2017)097

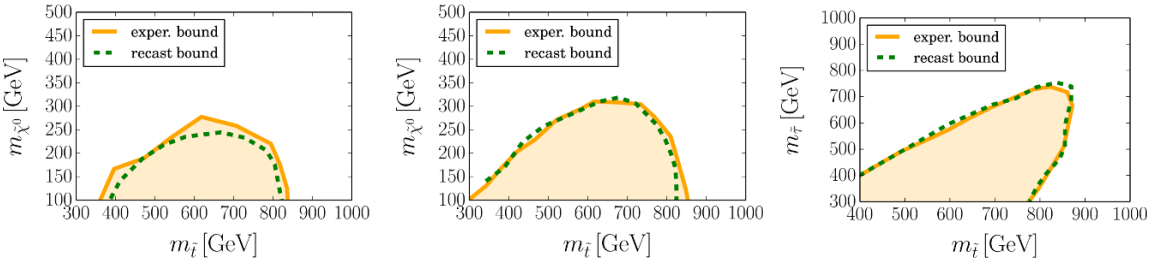

Figure 7. Comparison of the bounds reported by the experimental papers (solid orange lines) of ref. [39] (left panel), ref. [40] (middle panel) and ref. [41] (right panel) with those obtained after recasting the analyses (dashed green lines).

statistics (note that the analysis of ref. [41] is simply a counting experiment). The only caveat concerns the analysis of ref. [39]. The two signal regions considered in that search are not statistically independent. Therefore, the most constraining of the two statistics, each constructed out of the three bins of a particular signal region, is taken. Altogether, the comparison between the bounds reported in refs. [39–41] and ours are displayed in figure 7. We have checked that QCD next-to-leading order effects (taken as an overall K-factor) shift the dashed green lines by only a small amount.

References

[1] ALEPH collaboration, R. Barate et al., *Search for pair production of longlived heavy charged particles in e^+e^- annihilation*, *Phys. Lett.* **B 405** (1997) 379 [hep-ex/9706013] [INSPIRE].

[2] DELPHI collaboration, P. Abreu et al., *Search for heavy stable and longlived particles in e^+e^- collisions at $\sqrt{s} = 189$ GeV*, *Phys. Lett.* **B 478** (2000) 65 [hep-ex/0103038] [INSPIRE].

[3] OPAL collaboration, G. Abbiendi et al., *Search for stable and longlived massive charged particles in e^+e^- collisions at $\sqrt{s} = 130$ GeV to 209 GeV*, *Phys. Lett.* **B 572** (2003) 8 [hep-ex/0305031] [INSPIRE].

[4] L3 collaboration, P. Achard et al., *Search for heavy neutral and charged leptons in e^+e^- annihilation at LEP*, *Phys. Lett.* **B 517** (2001) 75 [hep-ex/0107015] [INSPIRE].

[5] R. Kopeliansky, *Search for charged long-lived particles with the ATLAS detector in pp collisions at $\sqrt{s} = 8$ TeV*, Ph.D. thesis, CERN-THESIS-2015-119, Technion Israel, (2015) [INSPIRE].

[6] CMS collaboration, *Search for long-lived charged particles in proton-proton collisions at $\sqrt{s} = 13$ TeV*, *Phys. Rev.* **D 94** (2016) 112004 [arXiv:1609.08382] [INSPIRE].

[7] ATLAS collaboration, *SUSY searches with the ATLAS detector*, ATL-PHYS-PROC-2017-005, CERN, Geneva Switzerland, (2017).

[8] CMS collaboration, M. Kazana, *Searches for supersymmetry with the CMS detector at the LHC*, *Acta Phys. Polon.* **B 47** (2016) 1489 [INSPIRE].

JHEP04(2017)097

[9] D.G. Cerdeno, C. Muñoz and O. Seto, *Right-handed sneutrino as thermal dark matter*, *Phys. Rev.* **D 79** (2009) 023510 [arXiv:0807.3029] [INSPIRE].

[10] C. Arina and M.E. Cabrera, *Multi-lepton signatures at LHC from sneutrino dark matter*, *JHEP* **04** (2014) 100 [arXiv:1311.6549] [INSPIRE].

[11] J. Guo, Z. Kang, J. Li, T. Li and Y. Liu, *Simplified supersymmetry with sneutrino LSP at 8 TeV LHC*, *JHEP* **10** (2014) 164 [arXiv:1312.2821] [INSPIRE].

[12] C. Arina, M.E.C. Catalan, S. Kraml, S. Kulkarni and U. Laa, *Constraints on sneutrino dark matter from LHC Run 1*, *JHEP* **05** (2015) 142 [arXiv:1503.02960] [INSPIRE].

[13] G.F. Giudice and R. Rattazzi, *Theories with gauge mediated supersymmetry breaking*, *Phys. Rept.* **322** (1999) 419 [hep-ph/9801271] [INSPIRE].

[14] A. Delgado, G. Nardini and M. Quirós, *The light stop scenario from gauge mediation*, *JHEP* **04** (2012) 137 [arXiv:1201.5164] [INSPIRE].

[15] F. del Aguila, M. Quirós and F. Zwirner, *Detecting E_6 neutral gauge bosons through lepton pairs at hadron colliders*, *Nucl. Phys.* **B 287** (1987) 419 [INSPIRE].

[16] P. Langacker, *The physics of heavy Z' gauge bosons*, *Rev. Mod. Phys.* **81** (2009) 1199 [arXiv:0801.1345] [INSPIRE].

[17] J. Scherk and J.H. Schwarz, *How to get masses from extra dimensions*, *Nucl. Phys.* **B 153** (1979) 61 [INSPIRE].

[18] I. Antoniadis, *A possible new dimension at a few TeV*, *Phys. Lett.* **B 246** (1990) 377 [INSPIRE].

[19] A. Pomarol and M. Quirós, *The Standard Model from extra dimensions*, *Phys. Lett.* **B 438** (1998) 255 [hep-ph/9806263] [INSPIRE].

[20] I. Antoniadis, S. Dimopoulos, A. Pomarol and M. Quirós, *Soft masses in theories with supersymmetry breaking by TeV compactification*, *Nucl. Phys.* **B 544** (1999) 503 [hep-ph/9810410] [INSPIRE].

[21] A. Delgado, A. Pomarol and M. Quirós, *Supersymmetry and electroweak breaking from extra dimensions at the TeV scale*, *Phys. Rev.* **D 60** (1999) 095008 [hep-ph/9812489] [INSPIRE].

[22] M. Quirós, *New ideas in symmetry breaking*, hep-ph/0302189 [INSPIRE].

[23] S. Dimopoulos, K. Howe and J. March-Russell, *Maximally natural supersymmetry*, *Phys. Rev. Lett.* **113** (2014) 111802 [arXiv:1404.7554] [INSPIRE].

[24] I. Garcia Garcia, K. Howe and J. March-Russell, *Natural Scherk-Schwarz theories of the weak scale*, *JHEP* **12** (2015) 005 [arXiv:1510.07045] [INSPIRE].

[25] A. Delgado, M. Garcia-Pepin, G. Nardini and M. Quirós, *Natural supersymmetry from extra dimensions*, *Phys. Rev.* **D 94** (2016) 095017 [arXiv:1608.06470] [INSPIRE].

[26] M. Carena, S. Gori, N.R. Shah, C.E.M. Wagner and L.-T. Wang, *Light stops, light staus and the 125 GeV Higgs*, *JHEP* **08** (2013) 087 [arXiv:1303.4414] [INSPIRE].

[27] T. Falk, K.A. Olive and M. Srednicki, *Heavy sneutrinos as dark matter*, *Phys. Lett.* **B 339** (1994) 248 [hep-ph/9409270] [INSPIRE].

[28] C. Arina and N. Fornengo, *Sneutrino cold dark matter, a new analysis: relic abundance and detection rates*, *JHEP* **11** (2007) 029 [arXiv:0709.4477] [INSPIRE].

JHEP04(2017)097

[29] PandaX-II collaboration, A. Tan et al., *Dark matter results from first* 98.7 *days of data from the PandaX-II experiment*, *Phys. Rev. Lett.* **117** (2016) 121303 [arXiv:1607.07400] [INSPIRE].

[30] LUX collaboration, D.S. Akerib et al., *Results from a search for dark matter in the complete LUX exposure*, *Phys. Rev. Lett.* **118** (2017) 021303 [arXiv:1608.07648] [INSPIRE].

[31] P.J. Fox, A.E. Nelson and N. Weiner, *Dirac gaugino masses and supersoft supersymmetry breaking*, *JHEP* **08** (2002) 035 [hep-ph/0206096] [INSPIRE].

[32] C. Arina, M. Chala, V. Martin-Lozano and G. Nardini, *Confronting SUSY models with LHC data via electroweakino production*, *JHEP* **12** (2016) 149 [arXiv:1610.03822] [INSPIRE].

[33] C. Han, J. Ren, L. Wu, J.M. Yang and M. Zhang, *Top-squark in natural SUSY under current LHC Run* 2 *data*, *Eur. Phys. J.* **C 77** (2017) 93 [arXiv:1609.02361] [INSPIRE].

[34] M. Drees and M.M. Nojiri, *Production and decay of scalar stoponium bound states*, *Phys. Rev.* **D 49** (1994) 4595 [hep-ph/9312213] [INSPIRE].

[35] S.P. Martin, *Diphoton decays of stoponium at the Large Hadron Collider*, *Phys. Rev.* **D 77** (2008) 075002 [arXiv:0801.0237] [INSPIRE].

[36] G.T. Bodwin, H.S. Chung and C.E.M. Wagner, *Higgs-stoponium mixing near the stop-antistop threshold*, *Phys. Rev.* **D 95** (2017) 015013 [arXiv:1609.04831] [INSPIRE].

[37] M. Carena, S. Gori, N.R. Shah, C.E.M. Wagner and L.-T. Wang, *Light stau phenomenology and the Higgs $\gamma\gamma$ rate*, *JHEP* **07** (2012) 175 [arXiv:1205.5842] [INSPIRE].

[38] G. Marandella, C. Schappacher and A. Strumia, *Supersymmetry and precision data after LEP*2, *Nucl. Phys.* **B 715** (2005) 173 [hep-ph/0502095] [INSPIRE].

[39] ATLAS collaboration, *Search for the supersymmetric partner of the top quark in the jets + $E_{\mathrm{T}}^{\mathrm{miss}}$ final state at $\sqrt{s} = 13$ TeV*, ATLAS-CONF-2016-077, CERN, Geneva Switzerland, (2016).

[40] CMS collaboration, *Search for direct top squark pair production in the fully hadronic final state in proton-proton collisions at $\sqrt{s} = 13$ TeV corresponding to an integrated luminosity of* 12.9 fb^{-1}, CMS-PAS-SUS-16-029, CERN, Geneva Switzerland, (2016).

[41] ATLAS collaboration, *Search for top-squark pair production in final states with two tau leptons, jets and missing transverse momentum in $\sqrt{s} = 13$ TeV pp-collisions with the ATLAS detector*, ATLAS-CONF-2016-048, CERN, Geneva Switzerland, (2016).

[42] D.S.M. Alves, J. Liu and N. Weiner, *Hiding missing energy in missing energy*, *JHEP* **04** (2015) 088 [arXiv:1312.4965] [INSPIRE].

[43] E. Conte, B. Fuks and G. Serret, *MadAnalysis* 5*, a user-friendly framework for collider phenomenology*, *Comput. Phys. Commun.* **184** (2013) 222 [arXiv:1206.1599] [INSPIRE].

[44] E. Conte, B. Dumont, B. Fuks and C. Wymant, *Designing and recasting LHC analyses with MadAnalysis* 5, *Eur. Phys. J.* **C 74** (2014) 3103 [arXiv:1405.3982] [INSPIRE].

[45] R. Brun and F. Rademakers, *ROOT: an object oriented data analysis framework*, *Nucl. Instrum. Meth.* **A 389** (1997) 81 [INSPIRE].

[46] M. Cacciari, G.P. Salam and G. Soyez, *FastJet user manual*, *Eur. Phys. J.* **C 72** (2012) 1896 [arXiv:1111.6097] [INSPIRE].

[47] A.L. Read, *Presentation of search results: the CL_s technique*, *J. Phys.* **G 28** (2002) 2693 [INSPIRE].

JHEP04(2017)097

[48] J. Alwall et al., *The automated computation of tree-level and next-to-leading order differential cross sections and their matching to parton shower simulations*, *JHEP* **07** (2014) 079 [arXiv:1405.0301] [INSPIRE].

[49] T. Sjöstrand, S. Mrenna and P.Z. Skands, *PYTHIA* 6.4 *physics and manual*, *JHEP* **05** (2006) 026 [hep-ph/0603175] [INSPIRE].

[50] F. Staub, *SARAH* 4*: a tool for (not only SUSY) model builders*, *Comput. Phys. Commun.* **185** (2014) 1773 [arXiv:1309.7223] [INSPIRE].

[51] W. Porod and F. Staub, *SPheno* 3.1*: extensions including flavour, CP-phases and models beyond the MSSM*, *Comput. Phys. Commun.* **183** (2012) 2458 [arXiv:1104.1573] [INSPIRE].

[52] M. Carena, G. Nardini, M. Quirós and C.E.M. Wagner, *The effective theory of the light stop scenario*, *JHEP* **10** (2008) 062 [arXiv:0806.4297] [INSPIRE].

[53] F. Capela and G. Nardini, *Hairy black holes in massive gravity: thermodynamics and phase structure*, *Phys. Rev.* **D 86** (2012) 024030 [arXiv:1203.4222] [INSPIRE].

[54] S. Clesse and J. García-Bellido, *The clustering of massive primordial black holes as dark matter: measuring their mass distribution with advanced LIGO*, *Phys. Dark Univ.* **10** (2016) 002 [arXiv:1603.05234] [INSPIRE].

[55] S. Bird et al., *Did LIGO detect dark matter?*, *Phys. Rev. Lett.* **116** (2016) 201301 [arXiv:1603.00464] [INSPIRE].

[56] S. McGaugh, F. Lelli and J. Schombert, *Radial acceleration relation in rotationally supported galaxies*, *Phys. Rev. Lett.* **117** (2016) 201101 [arXiv:1609.05917] [INSPIRE].

[57] G. Gelmini and P. Gondolo, *DM production mechanisms*, in *Particle dark matter*, G. Bertone ed., Cambridge University Press, Cambridge U.K., (2010), pg. 121 [arXiv:1009.3690] [INSPIRE].

[58] G. Nardini and N. Sahu, *Re-reheating, late entropy injection and constraints from baryogenesis scenarios*, arXiv:1109.2829 [INSPIRE].

[59] H.K. Dreiner, *An introduction to explicit R-parity violation*, *Adv. Ser. Direct. High Energy Phys.* **21** (2010) 565 [hep-ph/9707435] [INSPIRE].

JHEP04(2017)097